A Soft-Switching Zeta-Based AC-Link Universal Converter

Mojtaba Salehi
Department of Electrical and Computer Engineering
Northeastern University
Boston, MA, USA
salehi.mo@northeastern.edu

Mahshid Amirabadi
Department of Electrical and Computer Engineering
Northeastern University
Boston, MA, USA
m.amirabadi@northeastern.edu

Abstract— AC-link universal converters are relatively new topologies that can transfer power from different types of sources to various kinds of electrical loads. These converters provide higher reliability by employing small film capacitors instead of large electrolytic ones, which have higher failure rates than other power electronic components. Furthermore, when isolation is needed, universal converters can use compact high-frequency transformers rather than bulky line-frequency transformers. These converters extend the principles of the operation of DC-DC converters to DC-AC, AC-DC, and AC-AC power conversion systems. This paper proposes a soft-switching Zeta-based universal converter that can step up and step down the voltage in a wide range. Compared to Cuk-based converters, the link capacitor in this topology has a lower peak voltage. This paper discusses the principles of the operation of this converter. The performance of the proposed structure is evaluated through simulations in this paper.

Keywords— universal converter, ac-ac converter, rectifier, softswitching, Ćuk converter, buck-boost converter, Zeta converter, high-frequency ac link, zero voltage turn-on, zero current turn-off.

I. INTRODUCTION

Considering the growth of electric energy consumption and different types of electrical loads, the demand for reliable and efficient universal converters that can transfer electric power from different types of sources to different kinds of loads has risen. However, employing conventional DC-link power converters with expensive DC electrolytic capacitors may cause problems in the power grid and other reliability-demanding applications due to their frequent failures and short lifetime at high temperatures [1]-[3]. The other problem with DC-link converters is that galvanic isolation is typically provided by heavy and large low-frequency transformers.

AC-link universal converters have received increasing attention in recent years due to their unique characteristics. These converters extend the principles of operation of DC-DC converters to DC-AC, AC-DC, and AC-AC applications. Buckboost-based and Ćuk-based universal converters are the most well-known types of these AC-link converters [4]-[14].

A Buck-Boost-based universal converter uses an inductor at the link to transfer power. The inductor is exposed to a high current ripple to help minimize the size of the inductor [4]. By adding a small capacitor in parallel with the link inductor, softswitching is realized and the efficiency is improved [5]. All the switches in this converter benefit from zero voltage turn-on and soft turn-off. The main problem with this topology is the high link peak current, which contributes to higher conduction losses. In [6], a soft-switching Buck-Boost-based universal converter with reduced link peak current is presented to enhance the efficiency of the system. However, this converter experiences a long resonating time during which no power is transferred, and this can negatively affect the performance of the system. To reduce the duration of the resonating modes, four-quadrant switches can be used instead of two-quadrant switches [7]; however, this will double the number of switches. In [8], a bidirectional PWM Buck-Boost-based AC-AC converter, which requires three bulky inductors for the energytransferring process, is proposed. A Buck-Boost inverter is proposed in [9, 10] to increase the voltage gain in the Buck-Boost-based family of AC-link converters. However, they suffer from high current spikes and low efficiency. In [11], another single-stage three-phase Buck-Boost-derived inverter is introduced to increase the voltage gain. The main shortcoming of this inverter is that it needs a large inductor and suffers from low efficiency.

In Buck-Boost-based AC-link converters, achieving high efficiency is typically challenging. In all the above-mentioned configurations, an inductor is the main energy-transferring element, which reduces the overall power density of the system. To solve this problem, another family of universal converters named Ćuk-based universal converters is introduced where a small film capacitor is employed as the energy-transferring element. In [12], a parallel capacitive-link universal converter is proposed to reduce the current stress of switches and enhance efficiency. A Cuk-derived three-phase AC-AC converter that uses a small series film capacitor instead of an electrolytic one is presented in [13]. In [14], by adding a small inductor in series with the link capacitor, a soft-switching Ćuk-based PV inverter is developed. In this converter, all the switches benefit from zero current turn-off and soft turn-on. The problem with Ćukbased universal converters is that the link capacitor has a high peak voltage value. To solve this problem a soft-switching Zeta-based inverter and a SEPIC-based rectifier, in which the capacitor has a lower peak voltage are proposed in [15]. The AC side switches of these converters benefit from zero current turn-off and soft turn-on. Also, a Zeta-based rectifier and a Zeta-based AC-AC converter with a lower capacitive link peak voltage are presented in [16]. However, the proposed topology and operating principles can be used only in hard-switching applications.

This paper proposes a soft-switching Zeta-based universal converter that can be configured as a rectifier or an AC-AC converter. In this converter, the output side diodes benefit from zero current turn-off and soft turn-on. In addition, the input side switches benefit from zero voltage turn-on and soft turn-off. The proposed topology not only eliminates the bulky electrolytic capacitors but also increases power density by using lightweight high-frequency transformers instead of heavy line-frequency transformers when galvanic isolation is required. Compared to Ćuk-based universal converters, the Zeta-based universal converter has a lower link capacitor peak voltage.

This article is organized as follows: The topologies and operating principles are introduced in section II. After that, the simulation results are presented in section III. Finally, the paper is summarized in section IV.

II. OPERATING PRINCIPLES

The operation principles of the three-phase Zeta rectifier and the Zeta-based three-phase AC-AC converter are presented in parts (A) and (B) of this section, respectively.

A. Three-phase Zeta Rectifier

Fig. 1(a) shows the isolated soft-switching three-phase zeta rectifier. In this topology, the input inductor ($L_{\rm in}$), and link capacitors, C_1 and C_2 , transfer the power from the input to the output. A small resonating capacitor ($C_{\rm resonance}$) is connected in parallel with the inductor. The transformer is optional, and in the isolated converter, the isolation is provided with a high-frequency transformer (HFT). In non-isolated topologies, only one capacitor is needed instead of C_1 and C_2 .

The link voltage, link current, input inductor voltage, and the input inductor current waveforms during different modes are depicted in Fig. 1(b). In this figure, it is assumed that the reference current of phase A $(I_A^{\rm ref})$, is positive and has the maximum absolute value among three-phase input currents. The reference current of phases B $(I_B^{\rm ref})$ and C $(I_C^{\rm ref})$ are negative and the absolute value of $I_C^{\rm ref}$ is smaller than $I_B^{\rm ref}$. It is obvious that based on absolute values of input currents, different switching patterns need to be selected.

Each cycle has six main operating modes, including three power transfer modes and three resonating modes. In the first mode, power is transferred from the input inductor to the link capacitor through the DC-side diode (Fig. 2(a)). During this mode, input switches are off, and all unfiltered input currents are equal to zero. When the link capacitor is fully charged and the input inductor current becomes zero (Fig. 1(b)), the DC-side diode turns off under zero current switching (ZCS) condition and mode 2, which is a resonating mode, starts. During the first mode, the link capacitor voltage increases until its maximum value (Fig. 1(b)).

During mode 2, all switches are off, and the input inductor resonates with its parallel capacitor (Fig. 2(b)). At the end of this mode, the voltage of the input inductor reaches V_{AB} , and the voltages across switches Q_1 and Q_5 become zero to turn on these switches under zero voltage switching (ZVS) conditions.

During modes 2 and 3 (Figs. 2(b) and 2(c)), the link capacitor discharges to the DC load, and the link capacitor voltage decreases. Simultaneously, during mode 3, the input inductor charges from the input AC source with the second-highest line current. When the current of phase B (I_B) meets its reference value ($I_B^{\rm ref}$), switch Q_5 is turned off, and another resonating mode (mode 4) starts.

During mode 4 (Fig. 2(b)), the voltage across the DC-side diode is reverse-biased, so it cannot conduct, and the input inductor resonates with its parallel capacitor until the voltage across them becomes equal to V_{AC} . At this moment, switch Q_6 can turn on under ZVS, and mode 5 starts (Fig. 2(d)).

In mode 5, the input inductor charges from the input AC phase that has the lowest line current, and the link capacitor simultaneously continues discharging to the load. When the current of phase A (I_A) meets its reference value (I_A^{ref}) , the last power-transferring mode finishes, and the last resonating mode starts.

In mode 6, all switches are turned off and the input inductor resonates with its parallel capacitor. When the voltage of the input inductor becomes equal to the absolute value of the link voltage, the DC-side diode turns on with ZVS and the next cycle starts. It should be noted that the resonating modes are much shorter than the power transferring modes, but they are shown longer in Fig. 1(b) for more clarification.

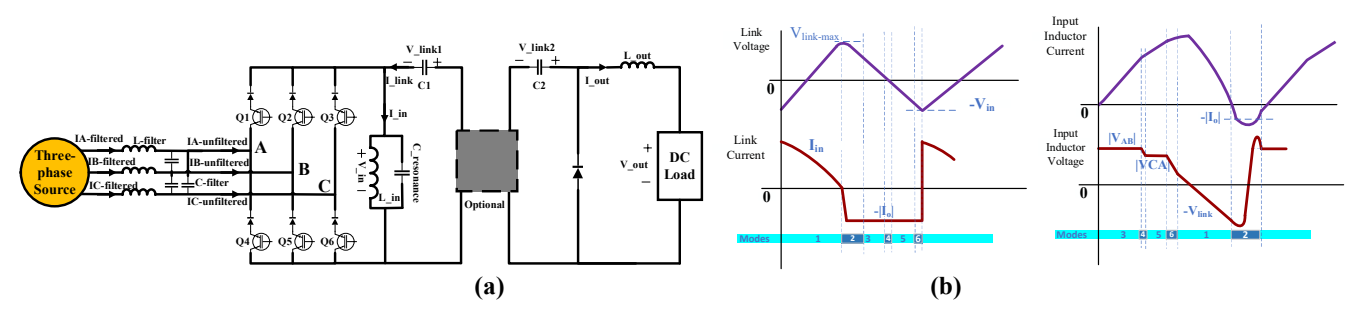


Fig. 1. (a) Isolated soft-switching Zeta-based three-phase rectifier (b) Link capacitor voltage, link capacitor current, input inductor current, and input inductor voltage waveforms in the Zeta-based rectifier.

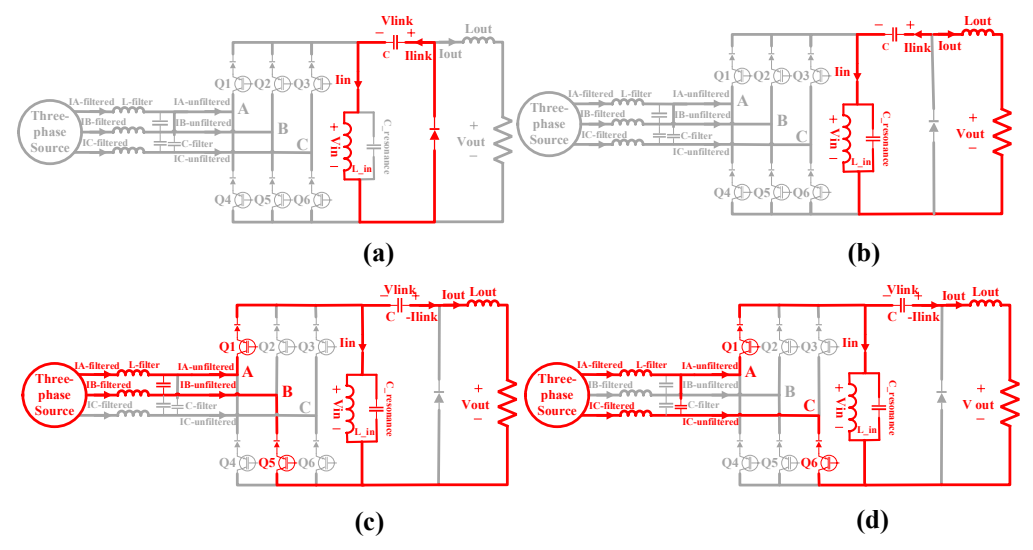


Fig. 2. Behavior of the non-isolated soft-switching three-phase AC to DC Zeta rectifier during (a) mode 1, (b) mode 2, mode 4, mode 6, (c) mode 5.

B. Zeta-Based Three-phase AC-AC Converter

Fig. 3 shows the isolated soft-switching three-phase AC-AC converter with a small film capacitor and an optional high-frequency transformer (HFT). The behavior of the proposed non-isolated soft-switching converter during different modes is shown in Fig. 4.

The first link capacitor charging mode and the two modes for charging the input inductor are like those of the zeta-based rectifier (Figs. 4(a), (e), and (f)). During the first mode, all the switches are off, and the power is transferred from the input inductor ($L_{\rm in}$) to the link capacitor ($C_{\rm link}$) via the output side antiparallel diodes. When the link capacitor is fully charged from the input inductor during the first mode, $I_{\rm in}$ becomes zero and diodes stop conducting under ZCS, and the resonating mode starts.

During the second mode, the input inductor resonates with its parallel capacitor (Fig. 4(b)) and the link capacitor starts to discharge to the load (Fig. 4(c)). This resonating mode lasts until when the input inductor voltage becomes equal to V_{AB} and provides zero voltage turn-on (ZVS) for the input-side switches to reduce power losses.

For link capacitor discharging modes, it is assumed that the voltage reference across the output phases AB $(V_{AB}{}^{\rm ref})$, is positive and has the maximum absolute value among three-phase output line-to-line voltages. The other line-to-line reference voltages are negative and the absolute value of the reference voltage across phases CA $(V_{CA}{}^{\rm ref})$ is smaller than the reference voltage across phases BC $(V_{BC}{}^{\rm ref})$. The polarities and values of the output line-to-line voltages determine which switches at the output side need to be turned on or off during each cycle.

It is also assumed that the reference current of phase A (I_A^{ref}) is positive and has the maximum absolute value among three-phase currents. The reference currents of phases B (I_B^{ref}) and C (I_C^{ref}) are negative and the absolute value of (I_C^{ref}) is smaller than

that (I_B^{ref}). Absolute values and current polarities determine zones and the input side switching pattern.

As depicted in Fig. 4(c), in the first discharging mode, the link capacitor is discharged to the three-phase load with the second-highest load current. During this mode, Q_7 , Q_{11} , and the anti-parallel diode of Q_9 conduct. When the corresponding output average line-to-line voltage ($V_{\rm BCo}$) meets its reference value ($V_{\rm BCo}$ ^{ref}), this mode ends, and the last discharging mode is initiated.

The last discharging mode discharges the link capacitor with the highest load current ($|I_{Ao}|$ in Fig. 4(d)). During this mode, Q_7 , Q_{11} , and Q_{12} are ON to supply the three-phase load. This mode lasts until the remaining energy of the link capacitor discharges to the load.

The first charging mode (Fig. 4(e)) starts after the first resonating mode. At the beginning of this mode, Q_1 and Q_5 start conducting under ZVS and the highest line-to-line voltage (V_{AB}) appears across the input inductor. As soon as the average value of the second-highest current (I_B) meets its reference value (I_B^{ref}), Q_5 turns off to initiate the second resonating mode.

In the second resonating mode, the input inductor and its parallel capacitor resonate and the voltage across the input inductor changes from V_{AB} to (V_{AC}) gradually. At the end of this mode, Q_6 turns on under ZVS to start the second inductor charging mode. And finally, during the second charging mode (Fig. 4(f)) line-to-line voltage (V_{AC}) appears across the input inductor to charge it. This mode continues until the average of I_C meets its reference value $(I_C^{\rm ref})$. At this point, the input switches turn off to initiate the last resonating mode. At the end of the last resonating mode, the input inductor voltage becomes equal to the absolute value of the link capacitor voltage to turn on the output-side anti-parallel diodes under ZVS for the next cycle.

It should be noted that the input inductor charging modes and the link capacitor discharging modes are controlled independently and they have different durations.

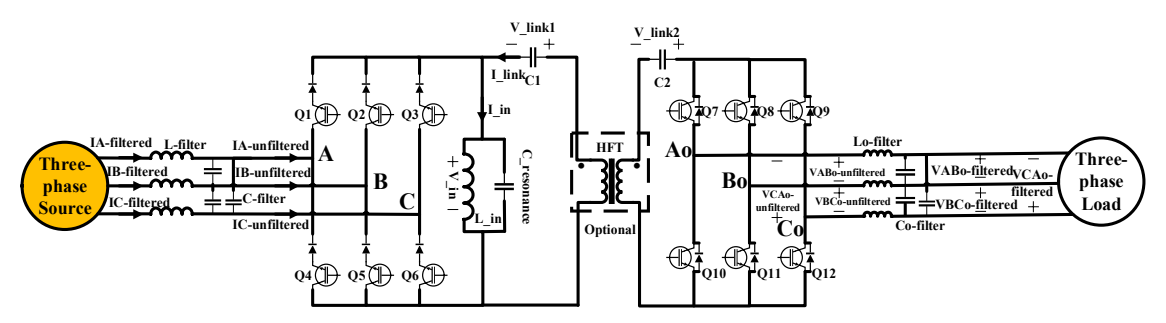


Fig. 3. Isolated soft-switching Zeta-based three-phase AC-AC converter.

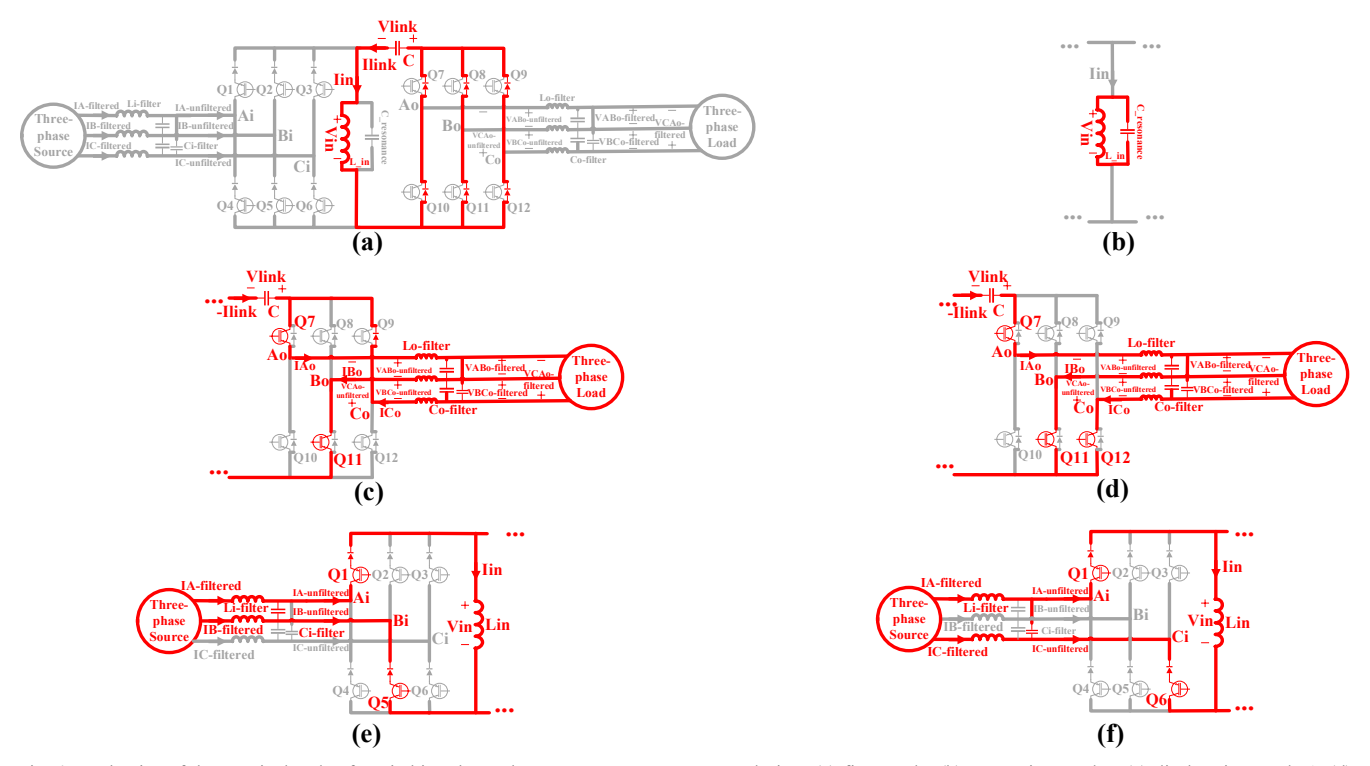


Fig. 4. Behavior of the non-isolated soft-switching three-phase AC-AC Zeta converter during: (a) first mode, (b) resonating modes, (c) discharging mode 1, (d) discharging mode 2, (e) charging mode 1, and (f) charging mode 2.

III. RESULTS

In this section, two simulation scenarios are carried out to verify the performance of the proposed rectifier and AC-AC converter. The parameters of these converters are summarized in Table I.

A. Soft-switching Zeta Rectifier

Simulation results corresponding to the proposed Zeta rectifier are shown in Figs. 5-9. Fig. 5 shows the voltage and current of the link capacitor. As it is evident, the link voltage is negative for a small portion of the cycle to allow using a small film capacitor with a lower voltage rating in comparison to Ćukbased converters. The measured link peak voltage is equal to 415 V, which is 100 V less than the Ćuk-based converter link peak voltage with the same parameters. Fig. 6 shows the input

inductor voltage and current waveforms. The input inductor's resonating modes, which facilitate soft-switching, can be seen in this figure.

The unfiltered input currents are depicted in Fig. 7. In Fig. 8, the currents and voltages of an input switch and the output diode are illustrated to verify the soft switching. It can be seen that the input switch has a zero-voltage turn-on and a soft turn-off. The DC-side diode benefits from a zero current turn-off and a zero-voltage turn-on. Fig. 9 shows the DC output voltage and three-phase filtered input current with a THD of 1.1%.

B. Soft-switching Three-phase AC-AC Zeta Converter

Simulation results corresponding to the designed three-phase AC-AC converter are illustrated in Figs. 10- 14. The voltage and current waveforms of the link capacitor are shown in Fig. 10. In this case, the link peak voltage is about 375 V which is less than

the Ćuk-based link peak voltage (475 V) simulated in the same condition. The input inductor current and voltage waveforms are illustrated in Fig. 11.

The unfiltered input currents and output voltages are depicted in Fig. 12. As mentioned in section II, the input inductor charging modes and the link capacitor discharging modes are controlled independently and they have different

durations. Fig. 13 shows the voltage and current of an input switch, which benefits from ZVS. For an output side antiparallel diode, the voltage and current waveforms show that these diodes benefit from ZCS and a ZVS at the end and beginning of mode 1, respectively (Fig. 13).

Fig. 14 shows the output filtered voltages with a THD of 3.6%, and the filtered input currents with a THD of 4.2%.

TABLE I. ZETA-BASED UNIVERSAL CONVERTER PARAMETERS

	Link frequency	Link capacitance	Input inductance	Resonance capacitance	Power level	Three-phase line-to-line input voltage amplitude	output voltage amplitude
Rectifier	25 kHz	300 nF	200 μΗ	10 nF	1 kW	175 V	200 V (DC)
AC-AC converter	5 kHz	1.8 μF	1 mH	200 nF	1 kW	200 V	180 V (line-to-line)

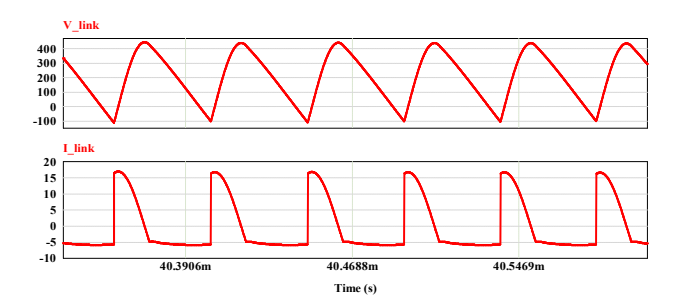


Fig. 5. Current and voltage of the link capacitor in the Zeta rectifier.

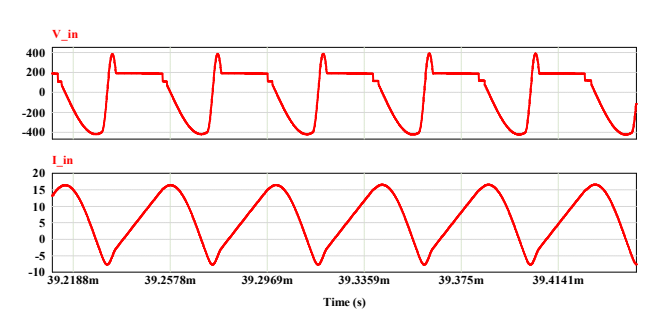


Fig. 6. Current and voltage of the input inductor in the Zeta rectifier.

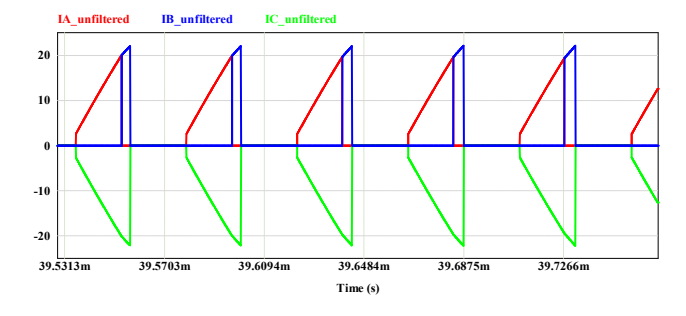


Fig. 7. Unfiltered input currents in the Zeta rectifier.

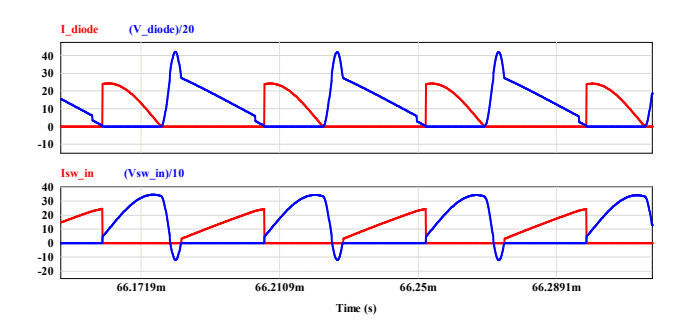


Fig. 8. Voltages and currents of the input and output switches in the Zeta rectifier.

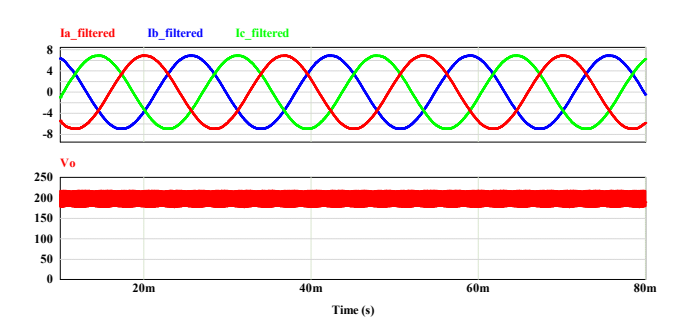


Fig. 9. Filtered input currents and output DC voltage in the Zeta rectifier.

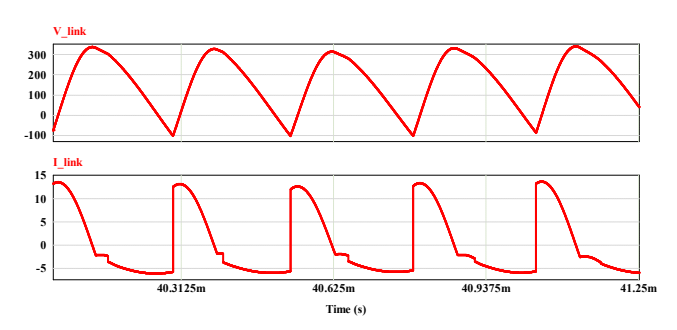


Fig. 10. Current and voltage of the link capacitor in the AC-AC Zeta converter.

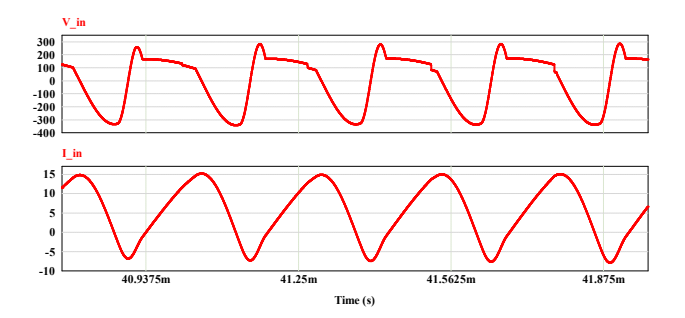


Fig. 11. Current and voltage of the input inductor in the AC-AC Zeta converter.

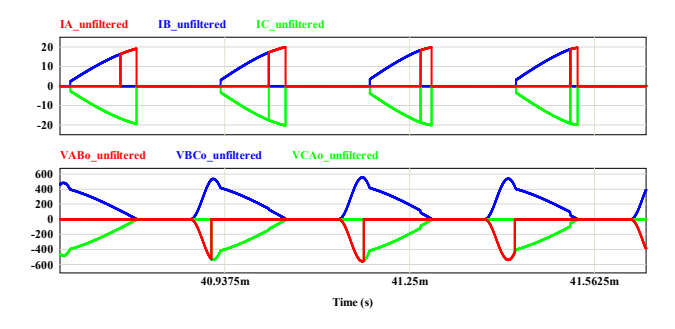


Fig. 12. Unfiltered input currents and unfiltered output voltages in the AC-AC Zeta converter.

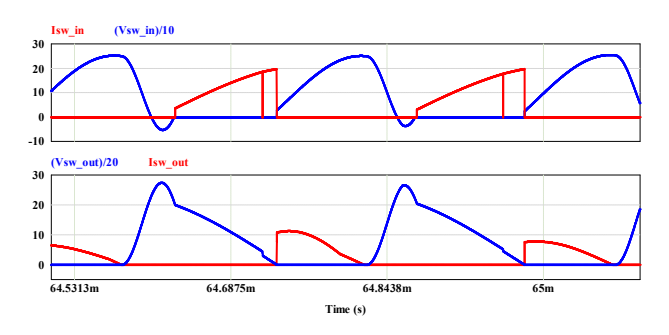


Fig. 13. Voltages and currents of the input switches and output anti-parallel diodes in the AC-AC Zeta converter.

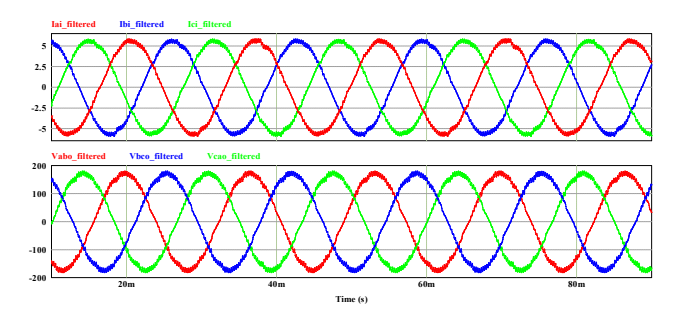


Fig. 14. Filtered output voltages and filtered input currents in the AC-AC Zeta converter.

IV. CONCLUSION

This paper presented a novel soft-switching zeta-based universal converter that can be configured as a three-phase rectifier or a three-phase AC-AC converter. In this topology, bulky unreliable electrolytic capacitors that are typically used in conventional DC-link converters, are replaced with small film capacitors. Furthermore, compared to Ćuk-based universal converters, the link capacitor peak voltage is decreased. In this converter, the output side diodes benefit from zero current turn-off and soft turn-on. And the input side switches benefit from zero voltage turn-on and soft turn-off. The proposed converter has the capability of using a high-frequency transformer instead of a bulky line-frequency transformer, which can reduce the total size and weight of the system.

ACKNOWLEDGMENT

This material is based upon work supported by the National Science Foundation under Grant No. 2047213.

REFERENCES

- C.-J. Shin and J.-Y. Lee, "An electrolytic capacitor-less bi-directional EV on-board charger using harmonic modulation technique," *IEEE Trans. Power Electron.*, vol. 29, no. 10, pp. 5195–5203, Oct. 2013.
- [2] H. Wang and F. Blaabjerg, "Reliability of capacitors for DC-link applications in power electronic converters—An overview," *IEEE Trans. Ind. Appl.*, vol. 50, no. 5, pp. 3569–3578, Sep./Oct. 2014.
- [3] T. Friedli, J. W. Kolar, J. Rodriguez, and P. W. Wheeler, "Comparative evaluation of three-phase AC-AC matrix converter and voltage DC-link back-to-back converter systems," *IEEE Trans. Ind. Electron.*, vol. 59, no. 12, pp. 4487–4510, Dec. 2012.
- [4] L. Kim and G. Cho, "New bilateral zero voltage switching AC/AC converter using high frequency partial-resonant link," in 16th Annual Conference of IEEE Industrial Electronics Society, 1990, pp. 857-862.
- [5] M. Amirabadi, J. Baek, H. A. Toliyat and W. C. Alexander, "Soft-Switching AC-Link Three-Phase AC-AC Buck-Boost Converter," in IEEE Transactions on Industrial Electronics, vol. 62, no. 1, pp. 3-14, Jan. 2015, doi: 10.1109/TIE.2014.2331011.
- [6] K. Mozaffari and M. Amirabadi, "A Highly Reliable and Efficient Class of Single-Stage High-Frequency AC-Link Converters," in IEEE Transactions on Power Electronics, vol. 34, no. 9, pp. 8435-8452, Sept. 2019, doi: 10.1109/TPEL.2018.2888583.
- [7] M. Amirabadi, H. A. Toliyat and W. C. Alexander, "A Multiport AC Link PV Inverter With Reduced Size and Weight for Stand-Alone Application," in IEEE Transactions on Industry Applications, vol. 49, no. 5, pp. 2217-2228, Sept.-Oct. 2013, doi: 10.1109/TIA.2013.2262093.
- [8] A. A. Khan, H. Cha, and H. F. Ahmed, "A new reliable three-phase buck-boost AC–AC converter," *IEEE Trans. Ind. Electron.*, vol. 65, no. 2, pp. 1000–1010, Feb. 2018.
- [9] F. Gao, P. C. Loh, R. Teodorescu, F. Blaabjerg, and D. M. Vilathgamuwa, "Topological design and modulation strategy for buck-boost three-level inverters," IEEE Transactions on Power Electronics, vol. 24, no. 7, pp. 1722-1732, 2009.
- [10] F. Gao, P. C. Loh, R. Teodorescu, and F. Blaabjerg, "Diode-Assisted Buck-Boost Voltage-Source Inverters," IEEE Transactions on Power Electronics, vol. 24, no. 9, pp. 2057-2064, 2009.
- [11] A. Darwish, A. M. Massoud, D. Holliday, S. Ahmed, and B. Williams, "Single-stage three-phase differential-mode buck-boost inverters with continuous input current for PV applications," *IEEE Trans. Power Electron.*, vol. 31, no. 12, pp. 8218–8236, Dec. 2016.
- [12] J. Luo, K. Mozaffari, B. Lehman and M. Amirabadi, "Parallel Capacitive-Link Universal Converters with Low Current Stress and High Efficiency," 2021 IEEE Energy Conversion Congress and Exposition (ECCE), 2021, pp. 2386-2393, doi: 10.1109/ECCE47101.2021.9595217.
- [13] E. Afshari, M. Khodabandeh and M. Amirabadi, "A Single-Stage Capacitive AC-Link AC-AC Power Converter," in IEEE Transactions on Power Electronics, vol. 34, no. 3, pp. 2104-2118, March 2019, doi: 10.1109/TPEL.2018.2841398.

- [14] M. Khodabandeh, E. Afshari, and M. Amirabadi, "A Single-Stage Soft-Switching High-Frequency AC-Link PV Inverter: Design, Analysis, and Evaluation of Si-Based and SiC-Based Prototypes," *IEEE Transactions on Power Electronics*, vol. 34, no. 3, pp. 2312-2326, 2018.
- [15] M. Khodabandeh and M. Amirabadi, "A Soft-switching Single-stage Zeta-/SEPIC-based Inverter/Rectifier," 2020 IEEE Applied Power Electronics Conference and Exposition (APEC), 2020, pp. 3456-3463.
- [16] M. Salehi, M. Khodabandeh and M. Amirabadi, "Zeta-Based AC-Link Universal Converter," 2022 IEEE Energy Conversion Congress and Exposition (ECCE), 2022, pp. 1-7, doi: 10.1109/ECCE50734.2022.9947744.